Brain Research Bulletin 207 (2024) 110879

Contents lists available at ScienceDirect

Brain Research Bulletin

journal homepage: www.elsevier.com/locate/brainresbull

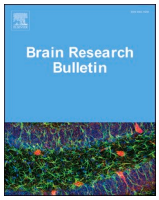

Research report

The seizure classification of focal epilepsy based on the network motif analysis☆

Denggui Fan [a], Lixue Qi [a], Songan Hou [b], Qingyun Wang [b,*], Gerold Baier [c]

[a] School of Mathematics and Physics, University of Science and Technology Beijing, Beijing 100083, China
[b] Department of Dynamics and Control, Beihang University, Beijing 100191, China
[c] Cell and Developmental Biology, University College London, London WC1E 6BT, United Kingdom

ARTICLE INFO

Keywords:
Focal seizures
Generalized seizures
Cortical motifs
Epileptor model

ABSTRACT

Due to the complexity of focal epilepsy and its risk for transiting to the generalized epilepsy, the development of reliable classification methods to accurately predict and classify focal and generalized seizures is critical for the clinical management of patients with epilepsy. In order to holistically understand the seizure propagation behavior of focal epilepsy, we propose a three-node motif reduced network by respectively simplifying the focal region, surrounding healthy region and their critical regions as the single node. Because three-node motif can richly characterize information evolutions, the motif analysis method could comprehensively investigate the seizure behavior of focal epilepsy. Firstly, we define a new seizure propagation marker value to capture the seizure onsets and intensity. Based on the three-node motif analysis, it is shown that the focal seizure and spreading can be categorized as inhibitory seizure, focal seizure, focal-critical seizure and generalized seizures, respectively. The four types of seizures correspond to specific modal types respectively, reflecting the strong correlation between seizure behavior and information flow evolution. In addition, it is found that the intensity difference of outflow and inflow information from the critical node (connection heterogeneity) and the excitability of the critical node significantly affected the distribution and transition of the four seizure types. In particular, the method of local linear stability analysis also verifies the effectiveness of four types of seizures classification. In sum, this paper computationally confirms the complex dynamic behavior of focal seizures, and the study of criticality is helpful to propose novel seizure control strategies.

1. Introduction

Focal epilepsy originates from a neural network confined to one hemisphere and is primarily classified as focal conscious seizures, focal impaired conscious seizures, and focal to bilateral tonic-clonic seizures (Ioannou et al., 2022; Lamy et al., 2022; Gauffin et al., 2022). Moreover, generalized epilepsy originates at a point within the bi-hemispheric distribution network. It rapidly becomes involved in the more comprehensive bilateral distribution network, with simultaneous bilateral seizures and synchronous epileptiform discharges as its main characteristics (Lamy et al., 2022; Gauffin et al., 2022; Bank et al., 2022). Focal seizures constitute 61% of the epilepsy population (Gupta et al., 2017). They are associated with high mortality, morbidity, economic burden, low quality of life, and high comorbidities (depression, anxiety, and cognitive impairment). Besides, surgery or stimulus treatment can cause severe side effects, particularly for drug-resistant populations. However, current treatments do not adequately address these issues, highlighting the need to develop new therapies for enhancing epilepsy management and reducing patients' economic burden.

A comprehensive understanding of the underlying cause of focal versus generalized seizures and the pathophysiologic mechanisms behind their interconversion remains a top priority. On the one hand, focal epilepsy can spread into generalized seizures. In addition to structural and genetic aetiologies, the neural networks and molecular pathologies involved in epileptogenesis are widely studied as epilepsy causes, e.g., the diagnosis of focal epilepsy may involve a variety of neural networks and is not limited to isolated brain regions (Raga et al., 2021). On the other hand, generalized epilepsy is inextricably linked to

☆ This work was supported by the National Natural and Science Foundation of China (Grants 12072021, 12372061, 12332004, and 11962019) and by the Fundamental Research Funds for the Central Universities and the Youth Teacher International Exchange & Growth Program (No. QNXM20220049).

* Corresponding author.
E-mail addresses: dgfan@ustb.edu.cn, nmqingyun@163.com (Q. Wang).

https://doi.org/10.1016/j.brainresbull.2024.110879
Received 23 August 2023; Received in revised form 10 December 2023; Accepted 13 January 2024
Available online 17 January 2024

focal seizures. It has been hypothesized that the focal theory may be a potential epileptogenic cause of primary generalized absence epilepsy, in which absence epilepsy is caused by the cortico-thalamic system (Ba-Armah et al., 2020). Moreover, focal epilepsy can also induce secondarily generalized absence seizures (Yang and Robinson, 2019). Seizures in infantile absence epilepsy (coexistence of generalized and focal epilepsy) may be caused by micro development of the local cortex or self-limited increased excitability in localized low-threshold regions (Yu et al., 2019). In some cases, despite significant advances in detection and imaging techniques, the pathophysiologic mechanisms underlying focal versus generalized seizures remain obscure (Lamy et al., 2022; Vaca and Park, 2020; Nascimento et al., 2023).

Accurately classifying patients with epilepsy as focal or generalized is one of the current clinical challenges (Chen et al., 2016; Aung et al., 2022). Traditionally, the International League Against Epilepsy (ILAE) indicates and characterizes the division between focal and generalized epilepsy by analyzing EEG signals. Primary generalized epilepsy is characterized by interictal epileptiform discharges with the highest and most extensive distribution on both sides of the brain (manifested as spikes and polyspikes with frequencies exceeding 3 Hz) (Panayiotopoulos et al., 1994). Focal epilepsy presents as seizures in only one brain region. Unfortunately, EEG categorization is far from satisfactory, and there is a risk that epilepsy key signatures will over- or under-interpret EEG findings (Vaca and Park, 2020; Nascimento et al., 2023; Aung et al., 2022). In modern times, machine learning techniques such as principal component analysis, independent component analysis, wavelet variational decomposition, adaptive mode decomposition, k-nearest neighbor (KNN), and Bayesian classifiers can be used to automatically identify and differentiate between focal and generalized epileptic seizures (Panayiotopoulos et al., 1994; Michelle et al., 2012). Despite the classification accuracy of the method, signal length, number of channels, and number of subjects significantly impact the results (Panayiotopoulos et al., 1994; Michelle et al., 2012; Luders et al., 1984). Overall, two types of pressing issues need to be addressed to improve classification accuracy. The first and foremost is blurring the boundary between focal and generalized epilepsy (Seneviratne et al., 2014). Due to multiple epileptic foci and the high likelihood of secondary seizures, there may be continuity between focal and generalized epilepsy (Vaca and Park, 2020; Bancaud et al., 1974). Also, focal EEG features have been found in generalized epilepsy (Vaca and Park, 2020; Aung et al., 2022; Kim et al., 2016). Secondly, there are effects of the nature of the EEG itself, such as differences in thresholds in waveform classification (Murariu et al., 2023; Lian et al., 2018). Therefore, further development of reliable neuroimaging-based assessment modalities is needed; otherwise, EEG signals can only be used as a classification aid for seizures (Raga et al., 2021).

Basic motifs in directed brain functional networks characterize the information flow of intrinsic activity and may reflect the synchronous excitation of functional modules in epileptic oscillatory networks (Bhattacharyya et al., 2018; Zhang et al., 2018). Cortical motifs represent networks' generalized categories and underlying generative processes (Gollo et al., 2014). The structural motifs of neuronal networks are the physical base of diverse functional information processing patterns. Functional motifs are distinct combinations of nodes and connections that can be selectively recruited or activated during neural information processing, and they are more prevalent in real brain networks. Cortical motifs permit the detection and comprehension of network topics and offer insight into the network's dynamic behavior (Wei et al., 2017). Three-node cortical motifs can effectively characterize how complex information flows evolve in brain networks. According to the theory of cortical foci, epileptic foci generate rapid and extensive epileptic discharges, and spatial interactions are associated with complex connectivity between cortical regions.

In addition, cortical patterning has a strong relationship with synchronization and delayed synchronization during epileptic seizures (Yang and Robinson, 2019; Aung et al., 2022). Mean field theory has also been utilized to examine the transition from focal to generalized seizures and their intrinsic dynamical (Bhattacharyya et al., 2018; Zhang et al., 2018; Sporns and Kötter, 2004). Therefore, beginning with the three-node cortical motifs, on the one hand, studying the composition of complex networks through smaller network building blocks can provide insights into the control laws of complex network structures. Then allow one to comprehend focal seizures' intrinsic information flow evolution mechanism fully. Cortical motifs, on the other hand, represent the structural and functional properties of genuine brain networks (Yang and Robinson, 2019). The same focal seizure may spread variably under distinct cortical motifs. Furthermore, whether it will expand into a full-blown seizure and to what extent is crucial to analyze. Combining cortical modalities with epilepsy dynamics modeling may therefore be a novel method for resolving the issue of focal seizure complexity and comprehending the information flow evolution and conversion mechanism in epileptic seizures.

This paper investigates a system consisting of a cortical motif and the Epileptor model for investigating seizure propagation and critical dynamics. The system possesses the spatial heterogeneity of focal epilepsy, incorporates focal, critical, and healthy regions, and simulates the propagation of focal seizures throughout the entire system. Further, the propagation of focal seizures and their underlying dynamic mechanisms were studied using seizure propagation marker values and local linear stability analysis. The findings suggest that the potential cause of focal seizures spreading into generalized seizures may be associated with the cortical primordium instead of the critical region. Moreover, this procedure considerably enhances the interpretation of complex focal seizures and may provide promising diagnostic biomarkers for clinical decision-making in epilepsy patients.

2. Materials and methods

2.1. Seizure and critical dynamics system

Large-scale neural networks are highly complex, notably directional complex networks; the complexity and diversity of information transmission directions and huge parameters can make it difficult for work to begin. Existing methods make it difficult and inefficient to explicitly examine the evolution of information flow. Therefore, it is necessary to identify a method that effectively reflects the overall characteristics while reducing the computational cost. In this paper, to fully understand the seizure propagation behavior of focal epilepsy as a whole, we compressed the focal region, the surrounding healthy region, and the critical region between them into three nodes and, based on these three nodes, constructed a model of seizure propagation. As shown in Fig. 1, the cortical motif dynamics analyses the evolution of critical dynamics for seizure propagation. Similarly, cortical motifs can frequently refine and categorize alterations in information flow, as depicted in Fig. 2**A**.

We constructed a seizure system (Fig. 2**B(a)**) for a preliminary qualitative analysis of whether focal seizures exhibit spreading behavior, considering the simplicity of the two-node cortical motif. Because the two-node cortical motif only comprises the focal and surrounding healthy regions, focal seizure transmission cannot be quantified in greater detail, and the transmission mechanism remains to be discovered. Consequently, based on the two nodes, we introduced a third node, a virtual node representing the critical region between the focal region and the surrounding healthy region, constituting the critical dynamical system (Fig. 2**B(b)**), corresponding to three-node cortical motifs. The three-node cortical motifs in Fig. 2**A** are identical to the network motifs detected in the mammalian brain (Wei et al., 2017), making this experiment more physiologically relevant and providing an excellent basis for comparison and thoroughness.

2.2. Epileptor dynamic model

We investigate networks with, N, nodes ($N = 2, 3$) whose dynamics

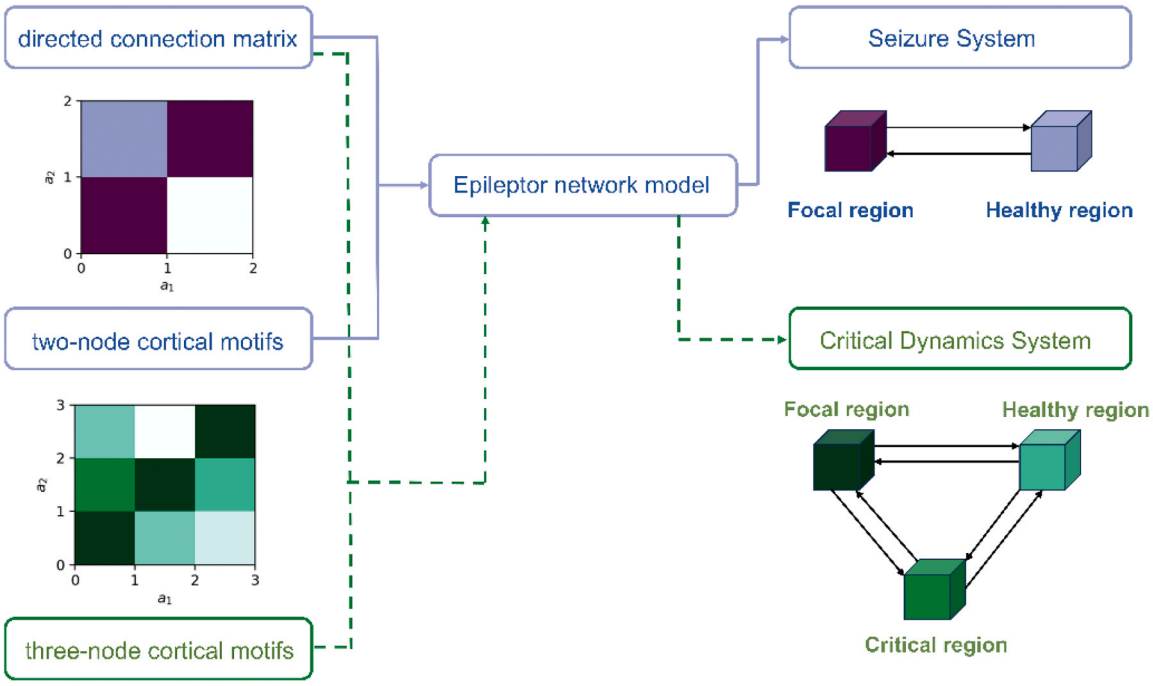

Fig. 1. Main flow diagram of the seizure and critical dynamics system. Seizure system: the directed connectivity matrix of the two-node cortical motif is input into the Epileptor model, including the focal and surrounding healthy regions. Critical dynamics system: A critical region is introduced between the focal and surrounding healthy regions. Again, based on the Epileptor model, the input is the directed connectivity matrix of the three-node cortical motif.

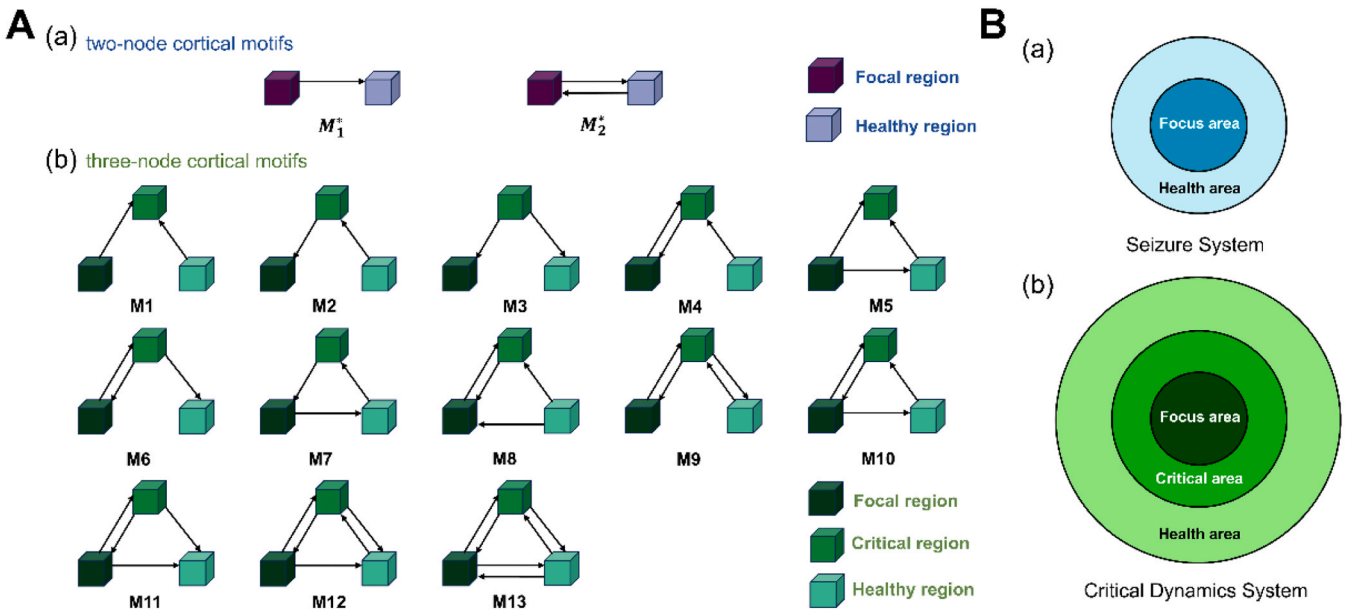

Fig. 2. Cortical motifs and seizure and critical dynamics systems are depicted in a schematic diagram. (A) Diagrammatic depiction of cortical motifs. (a) Cortical two-node motifs. M_1^*, refers to a two-node unidirectional cortical motif, whereas, M_2^*, refers to a two-node bidirectional cortical motif. The two specific nodes represent the focal and the surrounding healthy regions. (b) Cortical three-node motifs. The ordinal numbers M1 through M13 represent distinct connectivity patterns. The three separate nodes correspond, respectively, to the focal, critical and healthy regions. (B) Schematic of the system for seizure and critical dynamics. (a) The seizure system. (b) The critical dynamics system. Schematic representation of the containment relationship between specific focal, critical and healthy regions.

are described by the epileptor model (Jirsa et al., 2014), with, $i = 1,2,\ldots, N$. Table 1 lists the parameters considered in this paper.

Epileptor is a phenomenological model in which the physiological mechanism of seizure generation is replaced by the equivalent dynamic mechanism (Jirsa et al., 2014). It comprises one subsystem (subsystem 1) with two state variables (x_1&y_1) responsible for generating fast oscillations related to the potential activity of the neuronal membrane with the shortest time scale. And another subsystem (subsystem 2) has two state variables (x_2&y_2) generating SWE (sharp-wave events) and interictal spikes, with a slower time scale, τ_2, compared to subsystem 1, simulating the membrane potential. The variable, z_i, has the most significant time scale and represents the slowly varying permittivity variable responsible for guiding the two subsystems. During epileptic-like seizures, z_i is associated with slowly changing processes outside the cell,

Table 1
Main parameters of the Epileptor models.

Parameter	Meaning	Value
I_1	Passive current of subsystem 1	3.1
I_2	Passive current of subsystem 2	0.45
τ_0	Time scale of the permittivity variable	2857
τ_2	Time scale of subsystem 2	10
γ	Time constant in function $g(x)$	0.01
$x_{0,i}$	Excitability parameters of region i	$[-3.0, -1.0]$
w	Network Coupling Strength Threshold	20

such as ion levels, energy metabolism, oxygen content, etc. The function, $g(x_{1,i})$ is a low-pass filtered excitatory coupling from subsystem 1 to 2 to generate the SWE and interictal spikes. The function, $f_1(x_{1,i}, x_{2,i}, z_i)$, is a linear inhibitory coupling from subsystem 2 to 1. $f_2(x_{2,i})$ represents a linear suppression coupling between the two subsystems. The parameter, $x_{0,i}$, represents the neural excitability of the node as an "epileptic element" in the model that controls state switching, which can be used as the threshold to control the onset of the model (according to the current model, $x_{threshold} = -2.1$). When the $x_{0,i} > x_{threshold}$, the system will transit to the seizure phase.

$$\dot{x}_{1,i} = y_{1,i} - f_1(x_{1,i}, x_{2,i}, z_i) - z_i + I_1$$

$$\dot{y}_{1,i} = 1 - 5\dot{x}_{1,i} - y_{1,i}$$

$$\dot{z}_i = \frac{1}{\tau_0}\left[4(x_{1,i} - x_{0,i}) - z_i - w\sum_{j=1}^{N} W_{ij}(x_{1,j} - x_{1,i})\right]$$

$$\dot{x}_{2,i} = -y_{2,i} + x_{2,i} - x_{2,i}^3 + I_2 + 2g(x_{1,i}) - 0.3(z_i - 3.5) + \xi_i(t)$$

$$\dot{y}_{2,i} = \frac{1}{\tau_2}\left[-y_{2,i} + f_2(x_{2,i})\right] + \xi_i(t)$$

$$g(x_{1,i}) = \int_{t_0}^{t} e^{-\gamma(t-s)} x_{1,i}(s)ds$$

$$f_1(x_{1,i}, x_{2,i}, z_i) = \begin{cases} x_{1,i}^3 - 3x_{1,i}^2 & if \quad x_{1,i} < 0 \\ [x_{2,i} - 0.6(z_i - 4)^2]x_{1,i} & if \quad x_{1,i} \geq 0 \end{cases}$$

$$f_2(x_{2,i}) = \begin{cases} 0 & if \quad x_{2,i} < -0.25 \\ 6(x_{2,i} + 0.25) & if \quad x_{2,i} \geq -0.25 \end{cases} \tag{1}$$

In subsequent studies, in the two-node seizure system, the excitability of the focal region ($x_{0,1} = -1.6$) makes it has a seizure. At the same, the excitability of the healthy region ($x_{0,2} = -3.0$) makes it no seizure. Therefore, by regulating the characteristics of the system, it is possible to observe whether the healthy region that does not have seizures will be affected by focal seizures. Similarly, in the three-node critical dynamics research system, the excitability of regions is $x_{0,1} = -1.6, x_{0,2} = -3.0, x_{0,3} = -3.0$. The critical region is in a no-seizure state and less stable than the healthy one. Therefore, we can explore whether the critical region promotes focal seizure and then affects healthy regions, prevent its transmission, or reverses the health inhibitory information to prevent focal region seizure, which requires further exploration. Additionally, random white Gaussian noise, $\xi_i(t)$, is added to the model with mean 0 and standard deviation 0.05, and the time step of the numerical simulation is 0.01. In this model, $x_{1,i} + x_{2,i}$ can represent the electrographic signature of an epileptiform event and serve as initial data for the next section.

Suppose we want to combine cortical motifs with the model. In that case, we need to pay attention to the bidirectional connectivity of cortical motifs, so we replace the coupling weights with the directed connectivity matrix, W_{ij}. In the seizure system, the directed connectivity matrix is, $W_{two} = \begin{bmatrix} 0 & b_{fh} \\ b_{hf} & 0 \end{bmatrix}$. The abbreviation "$f$" stands for the focal region, "h" stands for the healthy region, and the front and back sequence represents the direction. For example, b_{fh} represents the connection strength from the focal region to the healthy region. Similarly, in the critical dynamics system, the directed connectivity matrix is, $W_{three} = \begin{bmatrix} 0 & a_{fc} & a_{fh} \\ a_{cf} & 0 & a_{ch} \\ a_{hf} & a_{hc} & 0 \end{bmatrix}$, where the abbreviation "f" stands for the focal region, the abbreviation "c" stands for the critical region, the abbreviation "h" stands for the healthy region, and the order from front to back represents the direction to point. For example, a_{cf} stands for the connection strength from the critical region to the healthy region. This is used to simulate various cortical motif patterns. Since the three-node cortical motif network contains six parameters, we classify four connection strength types for subsequent analysis and comparison to better quantify the overall changes and define multiple information flows. We make three connection strength parameters become a group (a_{fc}, a_{ch}, a_{fh}), representing the epileptogenic information flowing out from the focal region, which is defined as "forward." On the contrary, three connection strength parameters become the other group (a_{cf}, a_{hc}, a_{hf}), representing the information that prevents seizures from the healthy region, which is defined as "backward." After that, we define four connection strength types: I. forward=backward = 0.2; II. forward = 0.2, backward= 0.8; III. forward = 0.8, backward = 0.2; IV. forward=backward = 0.8, to explore the effect of the strong and weak relationship between the positive epileptogenic information flow and the negative seizure-preventing information flow on the outcome of seizure propagation.

2.3. Seizure propagation marker values

The time series containing seizures and the external influence of various noises are highly complex and irregular. The existing time series analysis methods misunderstand the noise and transient spikes as seizures. Therefore, to effectively distinguish seizures from non-seizures in a time series, we developed a seizure propagation marker value, $s_{\max}$, to index the intensity and timing of seizures in a time series. As shown in Fig. 3, the data used in this study comes from the simulation result, $x(t)$, generated by the epileptor model, but this method can also be used for real EEG data.

First, the time series of seizures usually have a vast amount of data, and hundreds of thousands of data make the analysis task even more difficult. Under the simulation of the Epileptor model, the seizure series contains 229888 data for 449 s with a time step of 512. First, we performed slice discretization. For the whole series, one point was selected for each interval of 100, and the difference between the maximum and minimum values ($x_{\max}, x_{\min}$) was calculated. The total amount of data after processing is 2298. In addition, for interval 100, we also performed a detailed sensitivity analysis to demonstrate its validity and persuasiveness (See Figs. S1 and S2).

$$x'(i) = x_{\max} - x_{\min}, \tag{2}$$

which not only retains the data characteristics but also shortens the data length. Secondly, we binarized the data to avoid the influence of noisy and non-useful data, specifically avoiding the interference of some no-seizure spikes and measuring the sudden transition of seizures. If the difference between the current and previous values is greater than 0.2, then the result is 1. Further, by choosing various differentials and sensitivity analysis, we verified that 0.2 is the preferred value for $s_{\max}$, (as shown in Fig. S3 and Fig. S4) getting

$$x'(i) = \begin{cases} 1, x'_{i+1} - x'_i > 0.2 \\ 0, x'_{i+1} - x'_i \leq 0.2 \end{cases} \tag{3}$$

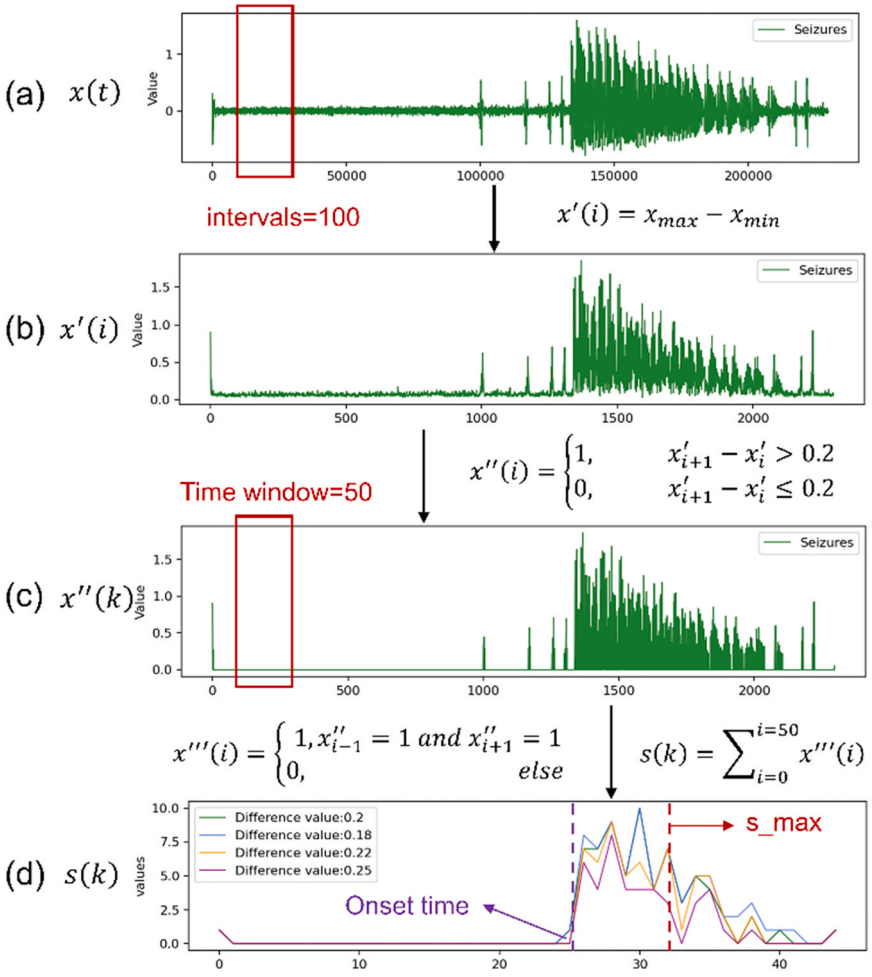

Fig. 3. The construct flowchart of seizure propagation marker value, s_{max}. (a) First, the simulation result of the epilepsy model is $x(t)$. (b) $x'(i)$, the difference between the maximum and minimum values within each interval. The interval is 100. (c) The inter-parameter, $x''(k)$. Data binarization: If the difference between the current and previous values is bigger than 0.2, the result is 1. Otherwise, the result is 0. (d) the degree of variation, $s(k)$. The Data binarization of inter-parameter $x'''(k)$. If the value of the previous and later moment is 1, the final value is 1; otherwise, the final value is 0. Secondly, sum all the values at every sliding window to get $s(k)$. The sliding window length is 50, and the overlap is 0. Finally, the maximum value of $s(k)$ is s_{max}. We mark the onset time of epilepsy as the previous time of value, which is the first value bigger than 0 in $s(k)$. The last word picture shows the processing results of selecting different difference values. In the end we chose 0.2.

Next, we perform another binarization to reflect the continuity of the oscillations during the seizure and avoid the influence of sudden short spikes during seizures. If the values of the previous and later moments are 1, then the final value is 1; otherwise, the final value is 0. Getting

$$x''(i) = \begin{cases} 1, x'_{i-1} = 1 and \quad x'_{i+1} = 1 \\ 0, otherwise \end{cases} \tag{4}$$

Likewise, to determine seizure persistence, we set the sliding window size to 50 and compute the sum of all values in each time window to obtain the degree of variation. Longer than 50 may ignore more detailed features, while shorter than 50 may not achieve our goal of reducing the amount of data and finding representative values for onset times and spikes. Therefore, by choosing different window values and sensitivity analyses, we verified that 50 was the best for s_{max}, as shown in Figs. S5 and 6. In addition, the overlap is chosen as 0 here. At the same time, we have verified that different overlap values have a relatively small impact on s_{max}, to ensure the accuracy of subsequent experiments. The specific sensitivity analysis is shown in Figs. S7 and 8.

$$s(k) = \sum_{i=0}^{i=50} x''(i), \tag{5}$$

Finally, the maximum value of $s(k)$ is s_{max}, and k is the sereval number of the sliding window. In addition, the time delay in different regions can also reflect the degree of spread of seizures to a certain extent. Therefore, we mark the onset time of epilepsy as the previous time of value, which is the first value bigger than 0 in $s(k)$. In order to demonstrate the validity of our designed flag value for the judgment of epilepsy, we implemented the same calculation procedure on the no-seizure time series generated by the epilepsy model. The results are shown in Fig. S9.

Various experiments have proved that the s_{max} value of the sequence without epileptic seizure is no more than 3. Therefore, in order to better classify and distinguish epileptic seizures, we define that if $s_{max} \leq 3$ it proves that the time series has no seizures, and if $s_{max} > 3$, it indicates that the time series has seizures, and the larger the value of s_{max}, the more severe the seizures. Furthermore, in our paper, the time-series output of each node in the epilepsy model can be assigned a value, s_{max}, which is a crucial metric for determining the spread of seizures. Meanwhile, the s_{max} can recognize the main feature of a seizure, which is sudden spike discharges lasting 1–2 s, which can be observed in the EEG. Also, we proved the robustness and reliability of the metric s_{max} after extensive experiments. In the future, responding to different other models and EEG data, we can adjust the threshold space of the metric to make it flexible to adapt to a wide range of tasks. Therefore, we comprehensively consider the seizure and spread of the entire system and define a new judgment value of seizure or non-seizure, $dif_{seizure}$.

In the seizure system, we set the marker value of the focal region to $s_{\max 1}$, which is obtained from the model simulation output time series. Similarly, the marker value of the healthy region is $s_{\max 2}$. Afterward, to distinguish numerically for subsequent statistical analysis, we correspond to different situations with different values of, $dif_{seizure}$ to quantify the degree of spread of focal seizures. $dif_{seizure} = -1$, neither focal nor healthy regions have seizures; $dif_{seizure} = 0$, only focal region have seizures; $dif_{seizure} = 2$, both focal and healthy regions have seizures. See Table 2 for details. Similarly, in the case of three-node system, the critical dynamics system sets the sign values of the focal, critical, and healthy regions as $s_{\max 1}, s_{\max 2}, s_{\max 3}$, respectively. Similarly, use $dif_{seizure}$ to quantify the degree of spread of focal seizures. $dif_{seizure} = 1$, no seizure in the focal, critical and healthy regions;$dif_{seizure} = 2$, only focal region seizures;$dif_{seizure} = 5$, only focal and critical regions seizures; $dif_{seizure} = 8$, focal, critical and healthy areas both seizures. See Table 3 for details.

2.4. Local linear stability analysis

In the previous section, we set the result-oriented flag value, $s_{\max}$, as the seizure propagation marker. Considering that if epileptic seizures occur, the system is unstable. Therefore, we use the Jacobian matrix of the state variables of the dynamical system to calculate all its eigenvalues and sort them by the size of the real part. The system is considered stable if the biggest real part is less than 0. Otherwise, it is unstable (Njitacke et al., 2019). Based on this, we perform a local linear stability analysis.

First, for a seizure system, we select a noiseless Epileptor model whose state variables are $x_{11}, x_{21}, z_1, y_{11}, y_{21}, g_1; x_{12}, x_{22}, z_2, y_{12}, y_{22}, g_2$, and the overall Jacobian matrix is J_{21}.

Then we calculate the biggest real part of the eigenvalues, E_{21}, to represent the global stability of the system. However, we wish to quantify the spread of seizures. In addition, we take only the portion, A_4, of the second node (healthy region) as the local Jacobian matrix, J_{22}, and calculate the biggest real part of the eigenvalues, E_{22}, to determine the local stability of the system. Similarly, the state variables of a three-node critical dynamical system are, $x_{11}, x_{21}, z_1, y_{11}, y_{21}, g_1; x_{12}, x_{22}, z_2, y_{12}, y_{22}, g_2; x_{13}, x_{23}, z_3, y_{13}, y_{23}, g_3$. J_{31} is the comprehensive Jacobian matrix. We calculate the biggest real part of the eigenvalues, E_{31}, to represent the global stability of the system.

Also, we adopt only the $\begin{bmatrix} B_5 & B_6 \\ B_8 & B_9 \end{bmatrix}$ of the second and third nodes (critical and healthy region) as the local Jacobian matrix, J_{32}, and computes the biggest real part of the eigenvalues, E_{32}, to represent the system's local stability. Consequently, the judgment can be broadly classified into three categories. There are no seizures if global system and local system is stable; The seizure is local if global system is stable and the local system is unstable; The seizure is global if both global system and local system is unstable. Similar to the previous section, we also provide the epileptic seizure judgment value, $dif_{seizure}$, and the corresponding criteria, which is shown in Table 4 and Table 5. Detailed formulas can be found from Eqs. (S1) and (S2) in the appendix A.

Table 2
Seizure judgment table of the seizure system. No seizure (NSE), Seizure (SE), No spread (NSP), and Spread (SP).

Seizure result	Spread result	Focal region	Health region	Judgment condition	$dif_{seizure}$
NSE	NSP	NSE	NSE	$s_{\max 1} \leq 3 \cap s_{\max 2} \leq 3$	-1
SE	NSP	SE	NSE	$s_{\max 1} > 3 \cap s_{\max 2} \leq 3$	0
SE	SP	SE	SE	$s_{\max 1} > 3 \cap s_{\max 2} > 3$	2

3. Results

3.1. A preliminary exploration of the spread of focal seizures

Several circumstances influence the extent and propagation of focal seizures, and the ultimate result of each seizure remains uncertain. Hence, the identification of the internal mechanism and external result via theoretical approaches will contribute to the following management of epilepsy, have possessed practical importance. In order to achieve this objective, firstly, we investigate the propagation of seizures from the focal region to the healthy region, as well as identifying the factors which are critical to this phenomenon. This paper analyzed alterations in the strength of connections and the excitability of regions within a seizure system.

First, within the unidirectionally connected cortical motif, M_1^*, the system had a different intensity and time delay. Fig. 4 depicts the recruitment of the healthy region into the secure system of, M_1^*. The connectivity strength of cortical motifs was proportional to the severity of seizures and inversely proportional to the time delay. Therefore, we hypothesized that focal seizures could spread to the whole system. However, these findings were constrained by unidirectional connectivity, resulting in fixed effects. In addition, the bidirectionally connected cortical motif, M_2^*, the system was analyzed. As shown in Fig. 5**A**, the influence of various significant parameters on focal seizure spread was also evaluated. When the forward and backward information transmission between focal and healthy regions were equal, the law of focal seizure spread followed diagonalization; i.e., if the excitability of the two regions increases equally, the focal seizures will spread to the whole system. Moreover, when the forward and backward connection strengths between regions were unequal, if the forward connection was strong, the excitability of the focal region, x_1, was decisive; otherwise, if the backward connection was strong, the excitability of the healthy region x_2, was decisive. When the backward connection was more significant, focal seizures were prevented, and the entire system was no seizures.

As a result of the mutual influence and check and balance of focal and healthy regions within the system, the exchange and evolution of information flow were complex, resulting in various spread results of focal seizures. In order to observe the seizure results as a whole, we classified them into three major categories: (1) The seizure information in the focal region may be insufficient in other regions, resulting in focal seizures termed focal seizures; (2) It may be because the prevent seizure information of other no-seizure regions is too strong and transmitted to the focal region, resulting in no seizure. Then the entire system does not seizure, termed inhibitory seizures; (3) Focal seizures result in the intense transmission of information to other regions, which leads to systemic seizures, termed generalized seizures. Tables 2 and 3 present the focal seizure spread results for the two-node seizure system, which are determined by the seizure propagation marker value, $s_{\max}$, and the local linear stability analysis, respectively.

In addition, numerical quantification was provided to facilitate statistical analysis. $dif_{seizure} = -1$, corresponds to inhibitory seizures, $dif_{seizure} = 0$, corresponds to focal seizures, and $dif_{seizure} = 2$, corresponds to generalized seizures. Fig. 5**B** depicts the results of the system's classification of focal seizures spread in response to changes in regional excitability, while Fig. 6 depicts the results which changes in connection strength. As a result, we observed that the degree of focal seizure dissemination was strongly correlated with system excitability and connection strength. Moreover, the transformation of focal seizures into generalized seizures was directly related to the intensity of the focal region excitability. In contrast, the transformation into inhibitory seizures was closely related to the stability of the healthy region. Using the two methods' results and theoretically, we confirmed the complex diversity of focal seizures and found that the local linear stability analysis was more sensitive to critical states (focal regions have seizures, but

Table 3
Seizure judgment table of the critical dynamics system. No seizure (NSE), Seizure (SE), No spread (NSP), and Spread (SP).

Seizure result	Spread result	Focal region	Critical region	Health region	Judgment condition	$dif_{seizure}$
NSE	NSP	NSE	NSE	NSE	$s_{max1} \leq 3 \cap s_{max2} \leq 3 \cap s_{max3} \leq 3$	1
SE	NSP	SE	NSE	NSE	$s_{max1} > 3 \cap s_{max2} \leq 3 \cap s_{max3} \leq 3$	2
SE	SP	SE	SE	NSE	$s_{max1} > 3 \cap s_{max2} > 3 \cap s_{max3} \leq 3$	5
SE	SP	SE	SE	SE	$s_{max1} > 3 \cap s_{max2} > 3 \cap s_{max3} > 3$	8

Table 4
Stability analysis table of the seizure system. No seizure (NSE), Seizure (SE), No spread (NSP), and Spread (SP).

Seizure result	Spread result	Focal region	Health region	Judgment condition	$dif_{seizure}$
NSE	NSP	NSE	NSE	$E_{21} < 0 \cap E_{22} < 0$	-1
SE	NSP	SE	NSE	$E_{21} \geq 0 \cap E_{22} < 0$	0
SE	SP	SE	SE	$E_{21} \geq 0 \cap E_{22} \geq 0$	2

healthy regions did not, orange area in Fig. 5**B** and green area in Fig. 6). Precisely, the seizure propagation marker value, s_{max}, that we devised can quantify seizures' intensity and time delay with a certain degree of rationality, laying a solid foundation for future complex systematic research.

3.2. Significant contribution of cortical motifs to classification of focal seizure spread

After preliminary research, we discovered that focal seizures could develop into various types but were limited to two regions and unable to detect more complex situations. In order to investigate seizure results in greater detail, we introduced a critical dynamic system for a comprehensive investigation of 13 cortical motifs. Specifically, we analyzed the spread results of focal seizures for each cortical motif under four kinds of connection strength, as depicted in Fig. 7. Initially, in Fig. 7**A**, based on the seizure propagation marker values, s_{max}, we determined four classes of seizure, judged by $dif_{seizure}$ and the specific meanings were shown in Table 6. It was possible that the seizure information transmitted by the focal region was insufficient to cause seizures in the healthy region or that the critical region transmits information to prevent the spread of epilepsy, thereby, blocking seizures. Consequently, we termed this type as a focal-critical seizure. Nonetheless, the local linear stability analysis in Fig. 7**B** only reflected three seizure results: focal seizures, inhibitory

Table 5
Stability analysis table of the critical dynamics system. No seizure (NSE), Seizure (SE), No spread (NSP), and Spread (SP).

Seizure result	Spread result	Focal region	Critical region	Health region	Judgment condition	$dif_{seizure}$
NSE	NSP	NSE	NSE	NSE	$E_{31} < 0 \cap E_{32} < 0$	1
SE	NSP	SE	NSE	NSE	$E_{31} \geq 0 \cap E_{32} < 0$	2
SE	SP	SE	SE	SE	$E_{31} \geq 0 \cap E_{32} \geq 0$	8

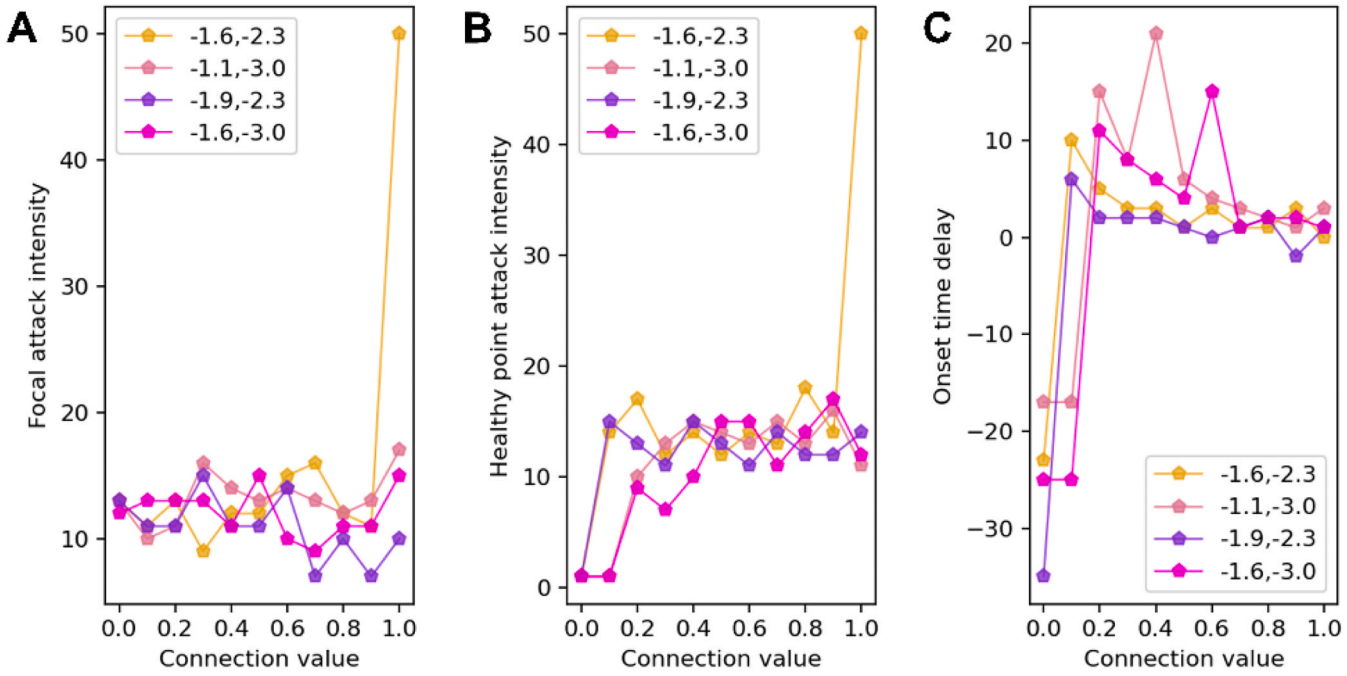

Fig. 4. Change plot of the leading indicators of the two-node cortical motif, M_1^*, system. (A) The focal region marker value, s_{max1}, varies with the connection strength, a_1, and a value less than three on the vertical axis indicates no seizure, otherwise seizure. (B) The healthy region marker value, s_{max2}, varies with the connection strength, a_1. (C) The onset time delay between the focal and healthy regions varies with the connection strength, a_1, where, a_1 is the magnitude of the connection strength from the focal region to the healthy region. Numbers in the legend represent excitability for focal and healthy regions. The four broken lines represent four different excitability values.

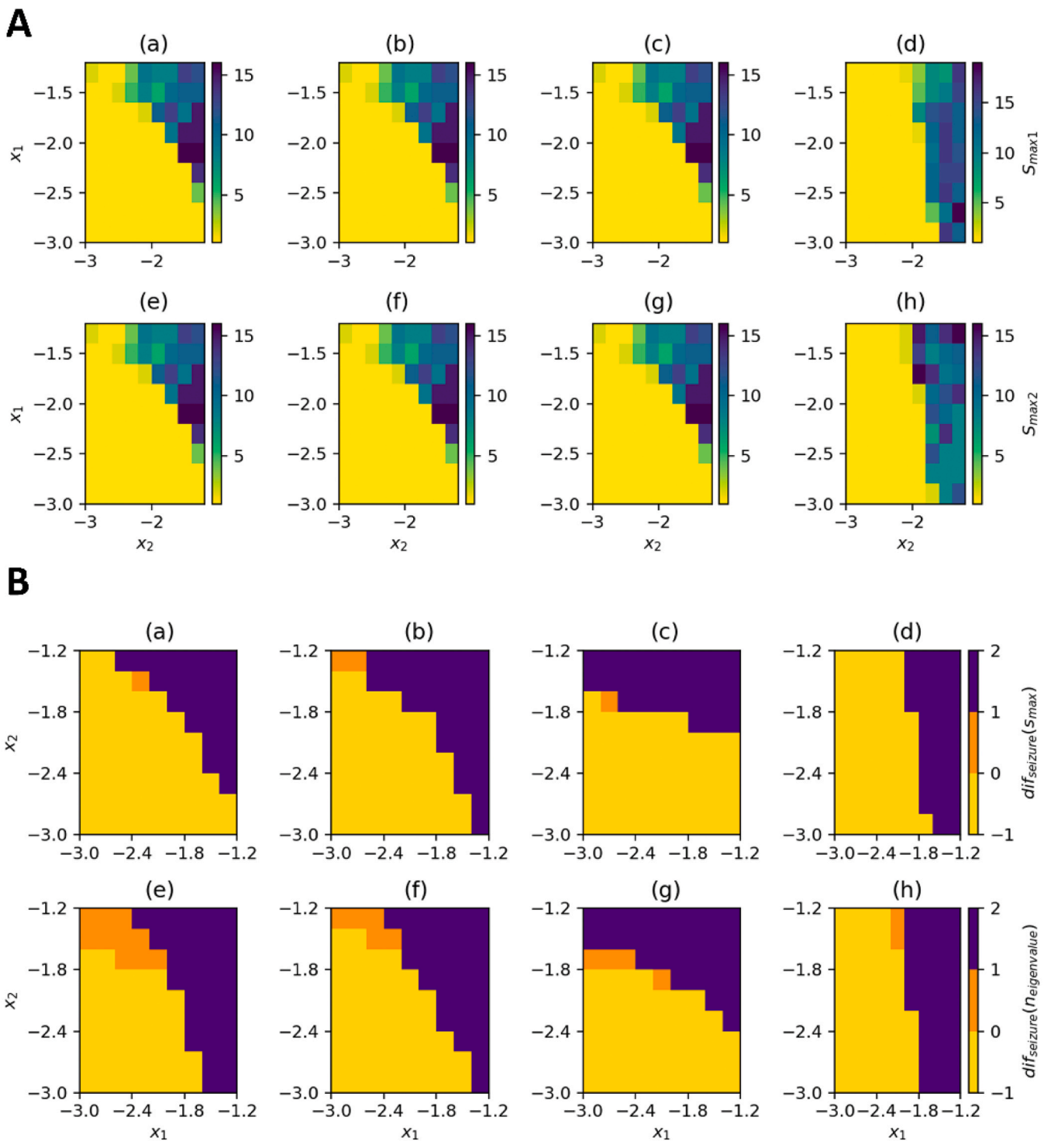

Fig. 5. Map of index changes in the seizure system of the two-node cortical motif, M_2^*. (A) (a–d) Excitability, x_1, in the focal region, x_2, in the healthy region, and seizure intensity of the focal region, $s_{\max 1}$, changes. (e-f) Excitability in the focal region, x_1, and, x_2, in the healthy region, and seizure intensity of the healthy region, $s_{\max 2}$, changes. a_{ch}: The connection strength from the focal region to the healthy region. a_{hc}: The healthy region points to the focal region. (a, e) $a_{ch} = a_{hc} = 0.2$. (b, f) $a_{ch} = a_{hc} = 0.5$. (c, g) $a_{ch} = 0.2, a_{hc} = 0.8$. (d, h) $a_{ch} = 0.8, a_{hc} = 0.2$. (B) The changes of the focal region excitability, x_1, the healthy region excitability, x_2, and seizure judgment value, $dif_{seizure}$. (a-d) $dif_{seizure}$, judged by the seizure marker value $s_{\max}$. (e-f) $dif_{seizure}$, judged by local linear stability analysis. a_{ch}: The connection strength from the focal region to the healthy region. a_{hc}: The healthy region points to the focal region. (a, e) $a_{ch} = a_{hc} = 0.2$. (b, f) $a_{ch} = a_{hc} = 0.5$. (c, g) $a_{ch} = 0.2, a_{hc} = 0.8$. (d, h) $a_{ch} = 0.8, a_{hc} = 0.2$. See Tables 2, 3 for definitions of, $dif_{seizure}$.

seizures and generalized seizures because the local stability was constituted of both the critical and healthy regions.

Different cortical motifs and categories of connection strength led to distinct results in focal seizure spread. In the condition M2 and M8 cortical motifs, seizures were consistently inhibited; In terms of the condition M1 and M4 cortical motifs, the class of seizure were prone to be focal-critical seizures; In the condition M5 and M11 cortical motifs, the class of seizure were more prone to be generalized seizures; and for

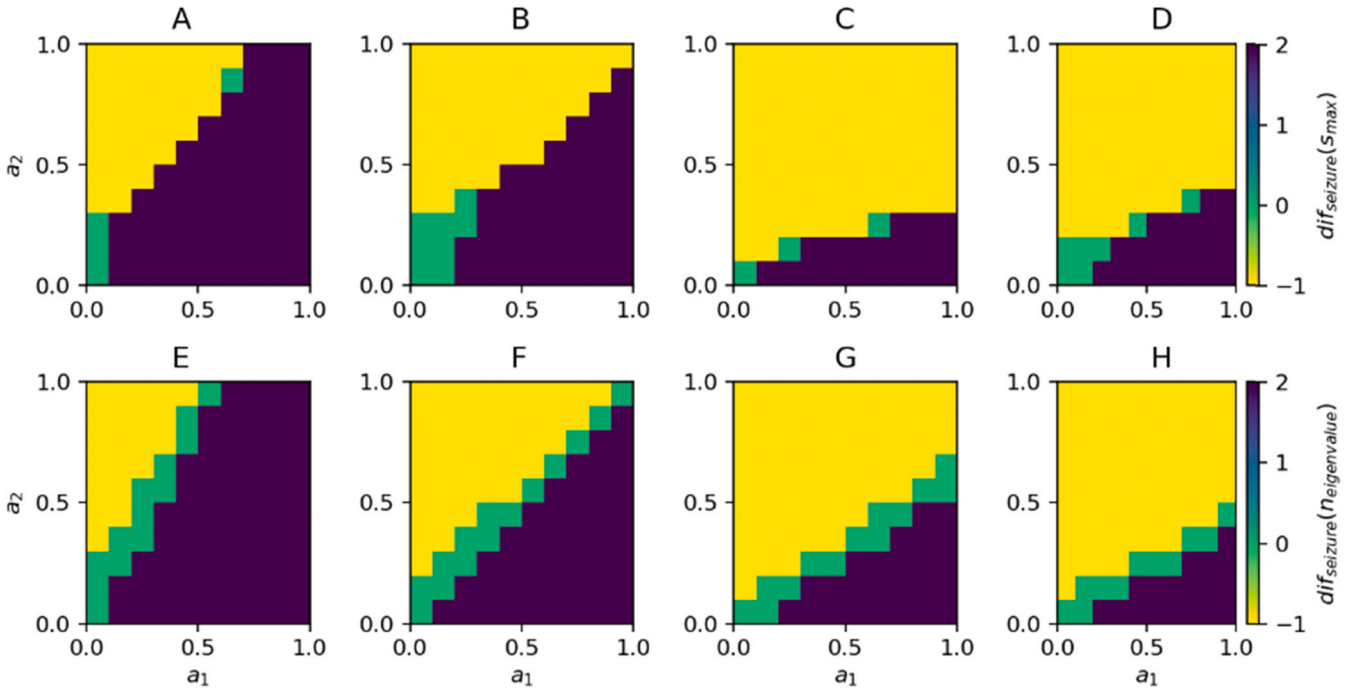

Fig. 6. Seizure judgment plot of connectivity strength variations in the seizure system of the two-node cortical motif, M_2^*. The changes of connection strength of the focal region and healthy region, a_{ch}, a_{hc}, and seizure judgment value, $dif_{seizure}$. (A-D) $dif_{seizure}$, judged by the seizure marker value, $s_{\max}$. (E-F) $dif_{seizure}$, judged by local linear stability analysis. x_1, represents the focal region excitability, and, x_2, represents the healthy region excitability. (A, E) $x_1 = -1.6, x_1 = -2.3$. (B, F) $x_1 = -1.1, x_2 = -3.0$. (C, G) $x_1 = -1.9, x_2 = -2.3$. (D, H) $x_1 = -1.6, x_2 = -3.0$. See Table 2, Table 3 for definitions of, $dif_{seizure}$.

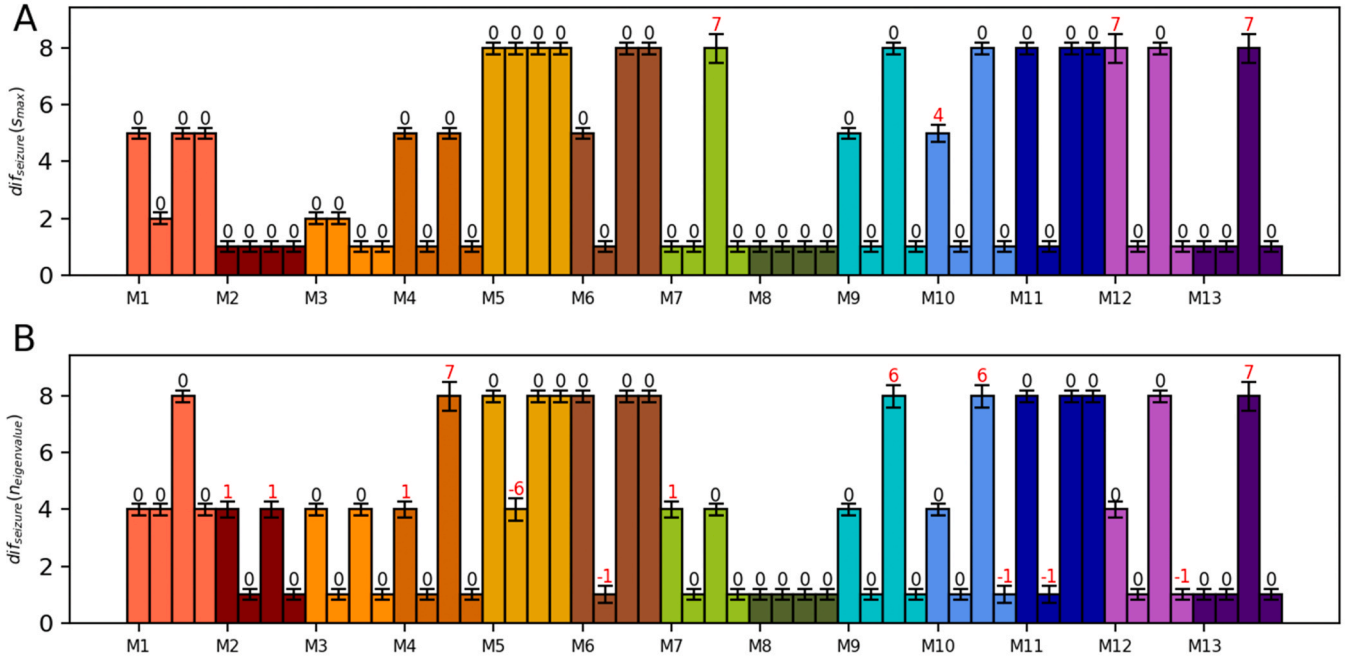

Fig. 7. The indicator statistics plot for the critical dynamical system of the three-node cortical motif. M1-M13 correspond to thirteen three-node cortical motifs corresponding to different column colors. The vertical axis is the seizure judgment value, $dif_{seizure}$. (A) The seizure value, $dif_{seizure}$, is judged by the seizure propagation marker values, $s_{\max}$. 1 indicates inhibitory seizures; 2 indicates focal seizures; 5 indicates focal-critical seizures; 8 indicates generalized seizures. The four bar graphs of every cortical motif correspond to four different categories of connectivity strength; see Methods for details. The error bars are represented as the difference between two sets of values for different connection strength types, the first being 0.2 for forward and 0.8 for backward, and the second being 0.4 for forward and 0.6 for backward. (B) Seizure value, $dif_{seizure}$, judged by local linear stability analysis. 1 indicates an inhibitory seizure, 4 indicates a focal seizure, and 8 indicates a generalized seizure. The rest of the description is the same as A.

Table 6
Seizure outcome classification table for 13 cortical motif systems (the seizure propagation marker values, s_{max}).

Connection	Inhibitory seizures	Focal seizures	Focal-critical seizures	Generalized seizures
C-type-1	M2,M7,M8,M13	M3	M1,M4, M6,M9, M10	M5,M11,M12
C-type-2	M2,M4,M6,M7, M8,M9,M10,M11, M12,M13	M1,M3	None	M5
C-type-3	M2,M3,M8	None	M1,M4	M5,M6,M7,M9, M10,M11,M12, M13
C-type-4	M2,M3,M4,M7, M8,M9,M10,M12, M13	None	M1	M5,M6,M11

case of M3, the system tended to maintain focal seizures. In addition, the results obtained based on s_{max} and local linear stability analysis were approximately the same, and the error of the former was minor. And the results maintained above was rarely affected by the connection strength between regions. This demonstrated the validity of our designed, s_{max}, value to some extent.

Thus far, we had concentrated on the spread effects of focal seizures, which could be broadly categorized into four categories.

(1) Inhibitory seizures (No seizures in the focal, critical and healthy regions).

(2) Focal seizures (Seizures only in the focal region).

(3) Focal-critical seizures (Seizures only in the focal and critical regions).

(4) Generalized seizures (Seizures in the focal, critical and healthy regions).

In particular, based on the seizure propagation marker values, s_{max}, we classified the focal seizure spread outcomes of the thirteen cortical motifs into four categories with each pie representing one of the four situations and four pie charts represent the four connection strength types Fig. 8**(A–D)**. We found that in connection strength type I (both forward and backward connections were weak), the distribution of the four epilepsy types was relatively even, indicating that seizure outcomes were more unpredictable. For connection strength type II (i.e., stronger backward connections), there were a high proportion of inhibitory seizures and no focal-critical seizures. For connection strength type III (i.e., stronger forward connections), there were a high proportion of generalized seizures, absence of focal seizures. Type IV (forward and backward connections equally strong), there were overt inhibitory seizures, and even focal seizures were absent. In general, inhibitory and generalized seizures were more prevalent, whereas focal and focal-critical seizures were ephemeral states that were more challenging to capture. If the connections backward were strong enough, focal-critical seizures would not occur. There might be unanticipated benefits if we could analyze its origins with precision. Similarly, local linear stability analysis methodologies produced comparable outcomes. However, due to the limitation of the Jacobian matrix's eigenvalues, there were only three cases in Fig. 8**(E–H)**, and focal-critical seizures could not be analyzed.

In conclusion, the properties of cortical motifs and the type of connection strength might determine the various diffusion outcomes of focal seizures; however, the nature and function of critical regions require further research. This might aid in the accurate classification of seizures and contribute to the classification of seizures in actual patients. The assignment of cortical motifs to seizure classification was detailed in Table 6 and Table 7**.**

3.3. *Mechanisms of critical region contribution to focal seizure spread*

In the preceding section, we discovered that the critical region

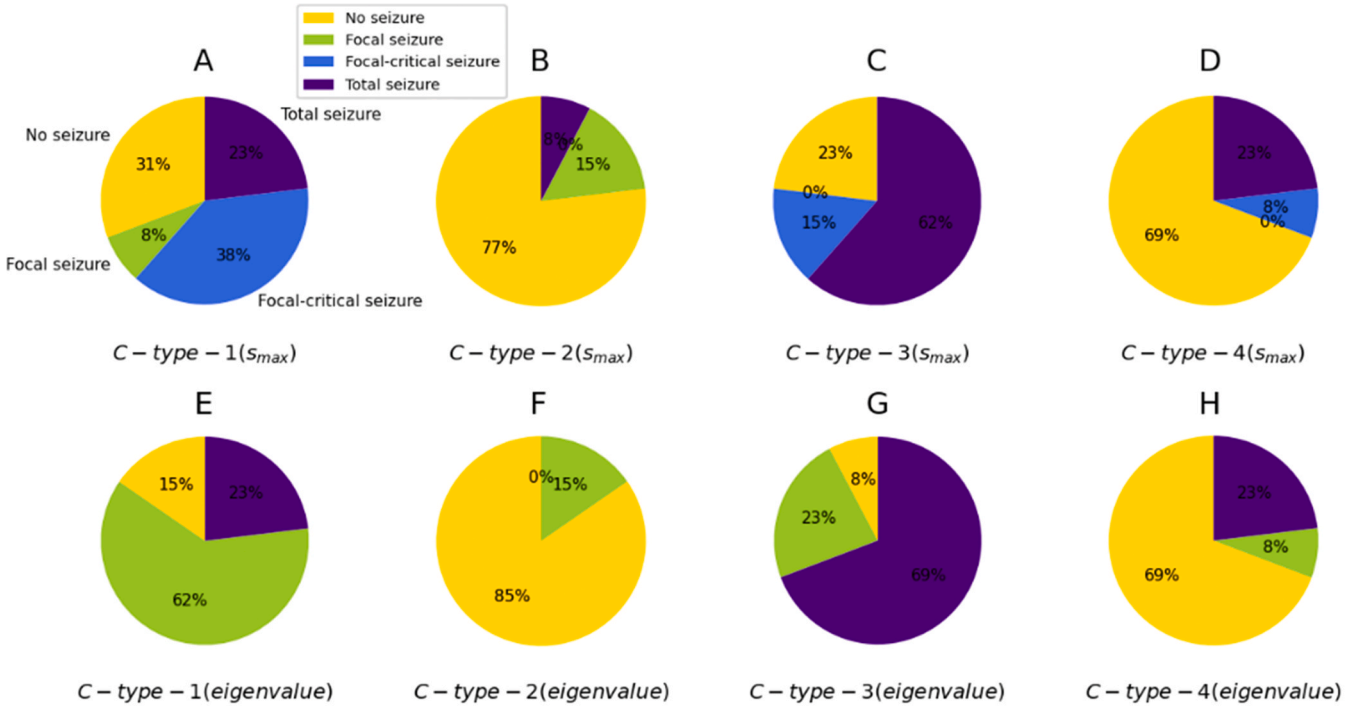

Fig. 8. Seizure-type classification map of 13 three-node cortical motifs. Percentages represent the ratio of cortical motifs per seizure type to the total number of thirteen. (A–D) The seizure judgment value, $dif_{seizure}$ for each cortical motif is determined from the seizure propagation marker values, s_{max}. According to the outcome value, four categories were classified: inhibitory seizures, focal seizures, focal-critical seizures, and generalized seizures. C-type-1 to C-type-4 represent four connection strength types. (E–H) Seizure judgment value, $dif_{seizure}$, for each cortical motif determined by local linear stability analysis. Results were classified into three categories: inhibitory, focal, and generalized.

Table 7
Seizure outcome classification table for 13 cortical motif systems (Local linear stability analysis).

Connection	Inhibitory seizures	Focal seizures	Generalized seizures
C-type-1	M8,M13	M1,M2,M3,M4, M7,M9,M10, M12	M5,M6,M11
C-type-2	M2,M3,M4,M6,M7, M8,M9,M10,M11, M12,M13	M1,M5	None
C-type-3	M8	M2,M3,M7	M1,M4,M5,M6,M9, M10,M11,M12,M13
C-type-4	M2,M3,M4,M7,M8, M9,M10,M12,M13	M1	M5,M6,M11

played a role in the propagation of focal seizures. In order to further investigate the role of critical regions in promoting or preventing seizures, we utilized changes in the properties of critical regions to clarify the role of various epilepsy categories. Adjustments were made to the excitability, x_2, the fast current, I_1, and the slow current, I_2, of the critical region in the epilepsy model, to observe variations in the spread results under various cortical motifs. Fig. 9, Fig. S10 and Fig. S11 illustrate the seizure judgment value, $dif_{seizure}$ of different excitability, x_2, the fast current, I_1, and the slow current, I_2 and combined with four connection strengths (see Method 2.2 for details).

The Results in conjunction with the four typical seizure types depicted in Fig. 8, we observed that the critical region properties of the system were classified by particular cortical motif. When the excitability of the critical region changed, the ultimate seizure outcomes would change. The connection strength types had impact on the evolution of seizures classes of different cortical motifs, which is shown by the four sub-plots corresponding to four connection strength types in Fig. 9. The excitability of the critical region might be an important factor governing the propagation of focal seizures, shown in Fig. 9**(A-D)**. In same motifs (M5, M8, M13), the seizure types kept the same along with the increment of the excitability of the critical region, x_2. In some motifs (M4, M9), the focal seizures would evolve to focal-critical seizures. In other motifs (M3, M6, M12), the inhibitory seizures would evolve to generalized seizures, some of which, would evolved to the intermediate date, the focal-critical seizures and certain excitability, x_2.

In addition, alterations in excitability were compared to previous classifications to demonstrate the reliability of our classification results. Then, particular cortical motifs, particularly highly stable ones, were investigated. Despite disparities in critical region excitability, M5 and M8 consistently exhibited generalized and inhibitory seizures across all four connectivity patterns. The focal-critical seizures usually evolved to the inhibitory seizures with a larger fast current, I_1, in the critical region in most cortical motifs (Fig. S10). In contrast, as the critical region's slow current, I_2, increased, most patterns shifted from inhibitory seizures to focal or focal-critical seizures (Fig. S11). Due to the specific values of the model parameters compared to physiology, our exploration of the connection between nodes is limited by other inherent parameters of the model, and there are still many issues that we cannot explore. The critical region might transmit both seizure information from the focal region and seizure prevention information from the healthy region. This might have tremendous potential if an effective strategy could be devised to amplify the inhibitory function of the critical region. However, the internal determinants of focal seizure propagation are highly complex, and the involvement of the critical region requires further investigation.

4. Discussion

Structural lesions such as abnormal brain development, extensive cortical malformations, brain tumors, vascular malformations, stroke, infectious and traumatic brain injury, metabolic disorders, and autoimmunity cause most known focal seizures (Nascimento et al., 2023). In addition, genetic causes, such as second brain somatic impingement or somatic mosaicism after fertilization only, can lead to focal seizures (Nascimento et al., 2023). Neonatal seizures in premature infants are associated with intraventricular hemorrhage and subsequent periventricular white matter degeneration, whereas the predominant injury in term infants is hypoxic-ischemic. Unfortunately, the pathogenesis is unknown in approximately 50% of facilities (Vaca and Park, 2020). Current extensive research on focal seizures demonstrates that making it

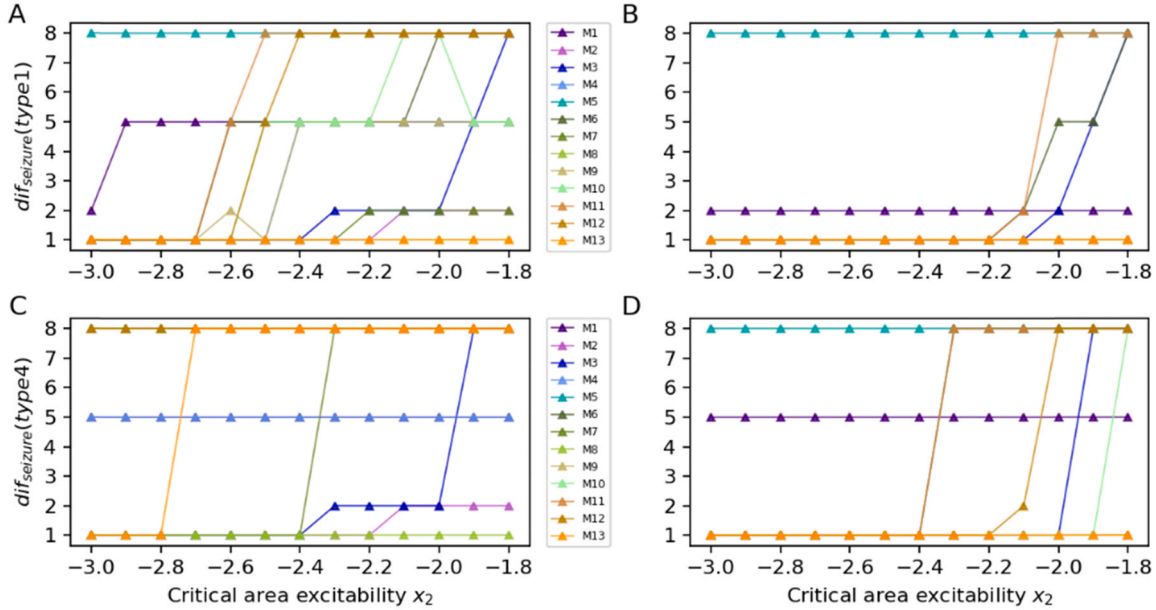

Fig. 9. Line graph depicting the relationship between seizure spread outcomes for 13 cortical motifs and the excitability of the critical region, x_2. Each of A-D represents a connection strength, the horizontal axis in each sub-plot represents the excitability of the critical region in the critical dynamics system, x_2, and the vertical axis is the seizure value, $dif_{seizure}$, the size, 1 indicates inhibitory seizures; 2 indicates focal seizures; 5 indicates focal-critical seizures; 8 indicates generalized seizures. Determine from the seizure propagation marker values, s_{max}. According to the legend, M1 to M3 corresponds to 13 topological patterns of cortical motifs. See method 2.2 for the specific four connection strength types.

is challenging to develop new treatments due to the quality of the assessment of the classification of seizure types in a given patient. Semiotics, neuroimaging, neurophysiology, and neuropathology are the pillars of diagnostic evaluation for epilepsy (Nascimento et al., 2023).

By modeling epileptic networks based on cortical motifs with focal spatial heterogeneity, our research examines how focal seizure spread can be classificated more meticulously and precisely. We discovered an interaction between the critical region's intrinsic properties and seizure type. Focal epileptic networks from the forebrain hemispheres may activate global epileptic networks in generalized seizures (Aung et al., 2022). This is consistent with our discovery that some focal seizures with cortical motifs convert to generalized seizures in the critical kinetic study system, specifically in some instances, such as generalized seizures with focal development (Lamy et al., 2022). Current research on the mechanisms of its genesis relies solely on the subjective, time-consuming, and inefficient explanations provided by neurologists under intense demands (Panayiotopoulos et al., 1994). In contrast, according to our theory, it is possible to discern this behavior by varying the regional excitability.

After meticulous consideration of seizure charismatics and diagnostic test results, such as video electroencephalogram (VEEG), neuroimaging, and genetic testing (Vaca and Park, 2020), a definitive diagnosis of focal and generalized seizures is made. MRI can detect minimal motor seizure abnormalities associated with consciousness loss (Raga et al., 2021; Baykan et al., 2011). It has been demonstrated that focal neuroimaging findings can be inaccurate (Ba-Armah et al., 2020), and those focal discharge syndromes are frequently misdiagnosed as focal seizures (Yu et al., 2019). Neuroimaging should not be used as the sole method to distinguish between focal and generalized seizures but rather as a supplementary method. Alternatively, we can combine actual brain computer data with multimodal data in the future to further refine our methods and conclusions. Nonetheless, it has been demonstrated that blending modalities can result in inaccurate feature extraction and classification (Murariu et al., 2023). In the future, we can incorporate inventive machine learning methods, such as integrated empirical modal decomposition and multivariate empirical modal decomposition (Murariu et al., 2023), to enhance the efficacy of combining actual multimodal data with our theoretical models.

From another angle, the wavelike processes revealed in the EEG exhibit linear and near-equilibrium dynamics at macroscopic scale, despite extremely nonlinear probably chaotic dynamics at microscopic scale (Robinson et al., 1997; Wright and Liley, 1996; Robinson et al., 2002; Bazhenov et al., 2008). The linear stability of large-scale brain dynamics can be used as a criterion to distinguish regular activity from epileptiform oscillations (Yang and Robinson, 2019). On the one hand, our current work integrates a dynamic model and local linear stability analysis for theoretical categorical distinctions, which may be more representative and circumvent the limitations of EEG signals. Clinical presentation is one of the most significant criteria for distinguishing between focal and generalized epilepsy. However, focal seizures are associated with a wide range of symptoms and clinical behaviors that are highly diverse (Raga et al., 2021). In the future, our work can also be integrated with clinical diagnosis to provide more pertinent direction.

In cognitive domains such as situational long-term memory, executive function, attention, working memory, visuospatial function, and language, focal and generalized epilepsy produce similar cognitive dysfunction. Moreover, patients with focal seizures have a reduced quality of life than those with generalized seizures (Raga et al., 2021). Patients with hereditary generalized epilepsy have impaired consciousness, cognitive and linguistic abilities, acquired knowledge, retrieval from long-term memory, and information processing (Andrade-Machado et al., 2021). However, the potential cognitive impairment disparities between focal and generalized seizures have not been thoroughly investigated (Raga et al., 2021).

Furthermore, the effective differentiation of seizure types in our research may allow for further examination of cognitive impairment in patients, thereby enhancing prevention and treatment. An underlying disease, genetic predisposition, structural alterations, antiepileptic medications, metabolic changes, disease duration, and seizure frequency may cause cognitive impairment. Our investigation of the mechanisms underlying the critical dynamics of seizures may also contribute to the potential etiology of cognitive impairment. Epilepsy of the temporal lobe with memory deficits, epilepsy of the frontal lobe with executive deficits and attention difficulties, and epilepsy of the parietal and occipital lobes with a decline in overall cognitive ability, memory, and executive functioning (Andrade-Machado et al., 2021; Yang et al., 2021). Currently, our work is based on a theoretical model. However, in the future, controlled modeling of various brain regions could be used to analyze the specific types of focal seizures further and assess cognitive impairment.

The current experiments have limitations, as the exploration of the virtual structure is limited to three nodes and only extends to the more extensive and complex whole brain network. Our method provides an initial correct guidance direction, in which the classification of the type of connection strength between forward and backward can reduce the complexity of the connection coefficients of the large-scale directed brain network. In addition, validation and incorporation of real-world data still need to be improved. However, the seizure propagation marker values, $s_{\max}$, we designed also apply to the actual EEG data time series. The current results indicate that age-concomitant comorbidities can muddy the distinction between focal and generalized seizures (Raga et al., 2021). We can match the theoretical model to actual data in the future. In that case, we can investigate the theoretical model's specificity and classify focal versus generalized seizures in patients with similar characteristics. Similarly, based on better-fitting theoretical models, the underlying etiology and pathogenesis of various seizures types can be analyzed in greater detail, as can the mechanisms underlying critical dynamics. In conclusion, we acknowledge the potential impact of these factors on classification performance, but our findings provide valuable insights into the future applicability of the method to real-world scenarios.

Epilepsy classification is used for ambiguous cases, neuromodulation, or surgical treatment options. Metabolic disorders are often associated with generalized rather than focal seizures \cite{nascimento2023focal}. Focal spikes associated with generalized epilepsy syndromes and childhood absence epilepsy do not require specific treatment in the focal absence (Nascimento et al., 2023). In patients with connectivity-rich focal spikes, especially in children, one does not want to miss the opportunity for epilepsy surgery, and patients are misclassified as having generalized epilepsy (Yu et al., 2019). Conversely, in patients with generalized epilepsy, one does not want to perform expensive preoperative epilepsy (Han et al., 2014). The diagnosis of focal versus generalized epilepsy determines the management of the patient, then the provision of optimal treatment and care. In surgical treatment, there are many problems with current neurosurgical resections, such as inconsistency between available histopathologic reports and clinical findings (Aung et al., 2022), and this paper helps in the preoperative evaluation of surgical resections for focal epilepsy based on theory. In medication, this paper helps select the right antiepileptic drug according to the specific seizure typology and circumvent the wrong choice of drug dosage, which can appear to aggravate seizures in a bad situation. Similarly, the results of this paper can give more detailed seizure regions and seizure types, which to some extent provide an additional data layer for correct diagnosis, which in turn reduces the cost of treatment and also helps to improve the treatment plan for patients with different epilepsy types and uncover the underlying pathophysiology of potential epileptic network alterations.

5. Conclusion

Based on a dynamic model of epilepsy, we investigated the fundamental dynamics underlying focal epileptic seizures in different cortical

subjects, where the evolutionary pattern of pattern transitions contributes to the categorical differentiation of epilepsy. We found that focal seizures can spread to varying degrees and even become generalized. Our approach broadly categorizes focal seizure propagation outcomes into four categories: inhibitory seizures, focal seizures, focal-critical seizures and generalized seizures. These four categories also apply to cortical motifs, representing the evolution and interaction of information flow and influenced by the type of connection strength. Inhibitory seizures and generalized seizures are more common. However, focal and focal-critical seizures are more difficult to capture; they may be transient. Finally, we exploit changes in the properties of critical regions to reveal the underlying dynamics of various epilepsy types. The main effects are the degree of excitation of critical regions and the intrinsic properties of cortical motifs. This provides neurologists with an invaluable tool to classify focal-seizure-spreading outcomes accurately, leading to more targeted and effective surgical interventions for epilepsy patients.

Author contribution

Denggui Fan: Proposed and supervised the project and contributed to writing the manuscript. Lixue Qi: Performed the experiments, wrote and revised the manuscript. Songan Hou: Assisted in the completion of the experiment and revised the manuscript. Qingyun Wang: Guided and supervised the manuscript. Gerold Baier: Guided and supervised the experiment and the manuscript.

CRediT authorship contribution statement

Qi Lixue: Writing – original draft, Visualization, Software, Data curation. **Fan Denggui:** Writing – original draft, Supervision, Methodology, Investigation, Funding acquisition, Formal analysis, Conceptualization. **Baier Gerold:** Supervision. **Wang Qingyun:** Supervision, Funding acquisition. **Hou Songan:** Writing – original draft, Investigation, Formal analysis.

Declaration of Competing Interest

The authors declared no potential conflicts of interest with respect to the research, authorship, and/or publication of this article.

Data availability

Data will be made available on request.

Appendix A. Supporting information

Supplementary data associated with this article can be found in the online version at doi:10.1016/j.brainresbull.2024.110879.

References

Andrade-Machado, R., Cuartas, V.B., Muhammad, I.K., 2021. Recognition of interictal and ictal discharges on EEG. Focal vs generalized epilepsy. Epilepsy Behav. 117, 107830.

Aung, T., Tenney, J.R., Bagić, A.I., 2022. Contributions of magnetoencephalography to understanding mechanisms of generalized epilepsies: blurring the boundary between focal and generalized epilepsies? Front. Neurol. 13, 831546.

Ba-Armah, D., Jain, P., Whitney, R., Donner, E., Drake, J., Go, C., Ochi, A., 2020. Misleading focal clinical, neurophysiologic, and imaging features in 2 children with generalized epilepsy who underwent invasive electroencephalographic (EEG) monitoring. J. Child Neurol. 35 (6), 418–424.

Bancaud, J., Talairach, J., Morel, P., Bresson, M., Bonis, A., Geier, S., Buser, P., 1974. "Generalized" epileptic seizures elicited by electrical stimulation of the frontal lobe in man. Electroencephalogr. Clin. Neurophysiol. 37 (3), 275–282.

Bank, A.M., Kuzniecky, R., Knowlton, R.C., Cascino, G.D., Jackson, G., Pardoe, H.R., Human Epilepsy Project Investigators, 2022. Structural neuroimaging in adults and adolescents with newly diagnosed focal epilepsy: the human epilepsy project. Neurology 99 (19), e2181–e2187.

Baykan, B., Altindag, E., Feddersen, B., Ozel, S., Noachtar, S., 2011. Does semiology tell us the origin of seizures consisting mainly of an alteration in consciousness? Epilepsia 52 (8), 1459–1466.

Bazhenov, M., Timofeev, I., Fröhlich, F., Sejnowski, T.J., 2008. Cellular and network mechanisms of electrographic seizures. Drug Discov. Today. Dis. Models 5 (1), 45–57.

Bhattacharyya, A., Sharma, M., Pachori, R.B., Sircar, P., Acharya, U.R., 2018. A novel approach for automated detection of focal EEG signals using empirical wavelet transform. Neural Comput. Appl. 29, 47–57.

Chen, P.C., Castillo, E.M., Baumgartner, J., Seo, J.H., Korostenskaja, M., Lee, K.H., 2016. Identification of focal epileptogenic networks in generalized epilepsy using brain functional connectivity analysis of bilateral intracranial EEG signals. Brain Topogr. 29, 728–737.

Gauffin, H., Landtblom, A.M., Vigren, P., Frick, A., Engström, M., McAllister, A., Karlsson, T., 2022. Similar profile and magnitude of cognitive impairments in focal and generalized epilepsy: a pilot study. Front. Neurol. 12, 746381.

Gollo, L.L., Mirasso, C., Sporns, O., Breakspear, M., 2014. Mechanisms of zero-lag synchronization in cortical motifs. PLoS Comput. Biol. 10 (4), e1003548.

Gupta, S., Ryvlin, P., Faught, E., Tsong, W., Kwan, P., 2017. Understanding the burden of focal epilepsy as a function of seizure frequency in the United States, Europe, and Brazil. Epilepsia Open 2 (2), 199–213.

Han, C.L., Hu, W., Stead, M., Zhang, T., Zhang, J.G., Worrell, G.A., Meng, F.G., 2014. Electrical stimulation of hippocampus for the treatment of refractory temporal lobe epilepsy. Brain Res. Bull. 109, 13–21.

Ioannou, P., Foster, D.L., Sander, J.W., Dupont, S., Gil-Nagel, A., Drogon O'Flaherty, E., Medjedovic, J., 2022. The burden of epilepsy and unmet need in people with focal seizures. Brain Behav. 12 (9), e2589.

Jirsa, V.K., Stacey, W.C., Quilichini, P.P., Ivanov, A.I., Bernard, C., 2014. On the nature of seizure dynamics. Brain 137 (8), 2210–2230.

Kim, D.W., Lee, S.Y., Lee, S.K., 2016. Focal epileptogenic lesions in adult patients with epilepsy and generalized epileptiform discharges. J. Epilepsy Res. 6 (2), 77.

Lamy, F., Valenti-Hirsch, M.P., Gauer, L., Gérard, B., Obeid, M., de Saint-Martin, A., Hirsch, E., 2022. Genetic generalized epilepsy and generalized onset seizures with focal evolution (GOFE). Epilepsy Behav. Rep. 19, 100555.

Lian, J., Liu, Z., Wang, H., Dong, X., 2018. Adaptive variational mode decomposition method for signal processing based on mode characteristic. Mech. Syst. Signal Process. 107, 53–77.

Luders, H., Lesser, R.P., Dinner, D.S., Morris, H.H., 1984. Generalized epilepsies: a review. Clevel. Clin. Q. 51 (2), 205–226.

Michelle, B., Pierre, G., Charlotte, D.2012. Epileptic syndromes in infancy, childhood and adolescence. John Libbey Eurotext.

Murariu, M.G., Dorobanțu, F.R., Tărniceriu, D., 2023. A novel automated empirical mode decomposition (EMD) based method and spectral feature extraction for epilepsy EEG signals classification. Electronics 12 (9), 1958.

Nascimento, F.A., Friedman, D., Peters, J.M., Bensalem-Owen, M.K., Cendes, F., Rampp, S., Beniczky, S., 2023. Focal epilepsies: update on diagnosis and classification. Epileptic Disord. 25 (1), 1–17.

Njitacke, Z.T., Kengne, J., Fozin, T.F., Leutcha, B.P., Fotsin, H.B., 2019. Dynamical analysis of a novel 4-neurons based Hopfield neural network: emergences of antimonotonicity and coexistence of multiple stable states. Int. J. Dyn. Control 7, 823–841.

Panayiotopoulos, C.P., Obeid, T., Tahan, A.R., 1994. Juvenile myoclonic epilepsy: a 5-year prospective study. Epilepsia 35 (2), 285–296.

Raga, S., Rheims, S., Specchio, N., Wilmshurst, J.M., 2021. Electroclinical markers to differentiate between focal and generalized epilepsies. Epileptic Disord. 23 (3), 437–458.

Robinson, P.A., Rennie, C.J., Wright, J.J., 1997. Propagation and stability of waves of electrical activity in the cerebral cortex. Phys. Rev. E 56 (1), 826.

Robinson, P.A., Rennie, C.J., Rowe, D.L., 2002. Dynamics of large-scale brain activity in normal arousal states and epileptic seizures. Phys. Rev. E 65 (4), 041924.

Seneviratne, U., Cook, M., D'souza, W., 2014. Focal abnormalities in idiopathic generalized epilepsy: a critical review of the literature. Epilepsia 55 (8), 1157–1169.

Sporns, O., Kötter, R., 2004. Motifs in brain networks. PLoS Biol. 2 (11), e369.

Vaca, G.F.B., Park, J.T., 2020. Focal EEG abnormalities and focal ictal semiology in generalized epilepsy. Seizure 77, 7–14.

Wei, Y., Liao, X., Yan, C., He, Y., Xia, M., 2017. Identifying topological motif patterns of human brain functional networks. Hum. brain Mapp. 38 (5), 2734–2750.

Wright, J.J., Liley, D.T.J., 1996. Dynamics of the brain at global and microscopic scales: neural networks and the EEG. Behav. Brain Sci. 19 (2), 285–295.

Yang, C., Liu, Z., Wang, Q., Luan, G., Zhai, F., 2021. Epileptic seizures in a heterogeneous excitatory network with short-term plasticity. Cogn. Neurodyn 15, 43–51.

Yang, D.P., Robinson, P.A., 2019. Unified analysis of global and focal aspects of absence epilepsy via neural field theory of the corticothalamic system. Phys. Rev. E 100 (3), 032405.

Yu, Y.L., Shi, M.T., Lu, H.J., 2019. Case of childhood absence epilepsy with focal spikes. World Neurosurg. 126, 601–604.

Zhang, L., Fan, D., Wang, Q., 2018. Synchronous high-frequency oscillations in inhibitory-dominant network motifs consisting of three dentate gyrus-CA3 systems. Chaos Interdiscip. J. Nonlinear Sci. 28 (6).